

Supplementary Information

An inorganic-organic composite framework with an unprecedented 3D heterometallic inorganic connectivity and white-light emission

**Huabin Zhang,^{a,b} Ping Lin,^a Xiaochen Shan,^{a,b} Fenglei Du,^{a,b} Qipeng Li^{a,b} and
Shaowu Du^{a*}**

^a *State Key Laboratory of Structure Chemistry, Fujian Institute of Research on the
Structure of Matter, Chinese Academy of Sciences, Fuzhou 350002, China. E-mail:
swdu@fjirsm.ac.cn.*

Fax: 86-591-83709470

^b *Graduate School of the Chinese Academy of Sciences, Beijing, 100049, China.*

Contents

1. Experimental procedures

1.1 Materials and Instruments.

1.2 Synthesis of compound $(\text{Me}_2\text{NH}_2)[\text{RbCd}_4(\text{OBA})_5]$ (**1**).

1.3 X-ray Crystallography

1.4 Synthesis and Characterization

2. Figures and Tables

Fig. S1 The coordination environment of metal centers in compound **1**. H atoms were omitted for clarity. Symmetry codes: (a) $1-x, -y, -z$, (b) $x, 0.5-y, 0.5-z$. (c) $1-x, -0.5+y, -0.5+z$. (d) $0.5-x, -y, z$. (e) $-0.5+x, 0.5-y, -0.5+z$. (f) $1-x, 1-y, -z$. (g) $x, 0.5-y, -0.5-z$.

Fig. S2 The coordination environment of ligands in compound **1**.

Fig. S3 View of the 3D inorganic network from the $[1\ 1\ 1]$ direction.

Fig. S4 View of $\{\text{Cd}_{16}\text{Rb}_4\}$ and $\{\text{Cd}_{18}\text{Rb}_2\}$ rings along separated axes. (a) $0.5+x, y, -z$. (b) $1+x, y, z$. (c) $1.5-x, 1-y, z$. (d) $1-x, 1-y, -z$. (e) $1-x, 0.5+y, 0.5+z$. (f) $0.5+x, 0.5-y, 0.5+z$. (g) $1.5-x, -y, z$. (h) $1+x, 0.5-y, -0.5-z$. (i) $1.5-x, 0.5+y, -0.5-z$. (j) $0.5+x, 1+y, -z$. (k) $1.5-x, 0.5+y, -0.5-z$. (l) $2-x, 0.5+y, 0.5+z$. (m) $2-x, 1-y, -z$. (n) $1+x, 1+y, z$.

Fig. S5 A polyhedral view (a) and a schematic representation (b) of $\{\text{Cd}_{16}\text{Rb}_4\}$ and $\{\text{Cd}_{18}\text{Rb}_2\}$ rings.

Fig. S6 IR spectrum of compound **1**.

Fig. S7. Simulated and experimental XRD powder patterns for compound **1**.

Fig. S8. TGA diagram for compound **1**.

Fig. S9 XRD, luminescent, IR and UV-adsorption spectra of compound **1** before and after excited by the portable UV-lamp for 2 h.

Fig. S10 Excitation spectra for the emissions at 427 and 566 nm in the solid state.

Fig. S11 The luminescence spectrum of the ligand (H_2OBA) at room temperature.

Fig. S12 MS analysis of **1** with ion current signals for $m/z = 18$.

Table S1 Pertinent crystal data and structure refinement results for **1**.

Table S2 The CIE coordinates of emissions excited at different wavelengths.

1. Experimental procedures

1.1 Materials and Instruments.

All the chemicals were purchased commercially and used as received. Thermogravimetric analysis-mass spectrometry analysis (TGA-MS) experiments were performed using a TGA/NETZSCH STA449C instrument heated from 30–1200 °C (heating rate of 10 °C /min, nitrogen stream). The powder X-ray diffraction (XRD) patterns were recorded on crushed single crystals in the 2θ range 5–50° using Cu-K α

radiation. The XRD were measured on a PANalytical X'pert PRO X-Ray Diffractometer. IR spectra using the KBr pellet technique were recorded on a Spectrum-One FT-IR spectrophotometer. Elemental analyses (C, H, and N) were measured with an Elemental Vairo EL III Analyzer. Fluorescence spectra for the solid samples were performed on an Edinburgh Analytical instrument FLS920.

1.2 Synthesis of compound (Me₂NH₂)[RbCd₄(OBA)₅]·H₂O (**1**).

A mixture of Cd(NO₃)₃·4H₂O (0.1542 g, 0.5 mmol), RbNO₃ (0.0589 g, 0.4 mmol) and H₂OBA (0.1290 g, 0.5 mmol) were placed in a 20 mL of Teflon-lined stainless steel vessel with 6 mL of mixed-solvent of MeOH (methanol) and DMF (N,N-Dimethylformamide) (V/V = 1:1). The mixture was heated to 145 °C in 4 h and kept to this temperature for 4 days. The reaction system was cooled slowly to room temperature during another 2 days. Colorless needle crystals of **1** were collected in 36% yield based on Cd(NO₃)₃·6H₂O. Elemental Anal. Calcd. for C₇₂H₄₆Cd₄NO₂₅Rb (1880.24): C, 46.49; H, 2.65; N, 0.75%. Anal. Found: C, 46.93; H, 2.35; N, 0.89%. IR: IR (KBr, cm⁻¹): 3399s, 3090s, 2965vw, 1945vw 1651m, 1590s, 1509s, 1381s, 1314vw, 1263vw, 1154w, 782 m, 728 m, 612vw. 782m, 728m, 612vw.

1.3 X-ray Crystallography.

Single-crystal X-ray diffraction data were collected on a Rigaku diffractometer with a Mercury CCD area detector (Mo K α ; $\lambda=0.71073\text{\AA}$) at room temperature. Empirical absorption corrections were applied to the data using the Crystal Clear program. The structures were solved by the direct method and refined by the full-matrix least-squares on F^2 using the SHELXTL-97 program. Metal atoms in each compound were located from the E -maps and other non-hydrogen atoms were located in successive difference Fourier syntheses. All non-hydrogen atoms were refined anisotropically. The (Me₂NH₂)⁺ cation is treated with a disordered model with 0.5 occupancy. The organic hydrogen atoms were positioned geometrically, while those of the counterions were located using the difference Fourier method and refined freely. MS analysis of **1** reveals that a mass fragment of 18 m/z corresponding to a H₂O molecule has been observed in the range of 100 to 300 °C (Fig S12), which supports the fact that there exists only one water guest molecule in the framework. This is

further confirmed by TGA, which show a weight loss for one water molecule. Considering the existence of two solvent accessible voids, this lattice water molecule is treated disordered over two positions each with occupancy of 0.5. Crystallographic data and other pertinent information are summarized in Table S1.

1.4 Synthesis and Characterization

Solvothermal synthesis has been proven to be a useful synthetic technique for the preparation of MOFs. The high temperature and pressure during these reactions can dramatically enhance the ligand solubility and the reactivity of reactants. With the aid of controlling the pH value of a solution and the temperature decreasing rate, as well as the appropriate choice of solvents and templates, crystallization of the products with different structural types can be achieved. The PH value is very important for the assembly of the title compound. High PH value may lead to the hydrolysis of metal ions while low PH value will decrease the coordination ability of the poly-carboxylic ligand. In addition, for Cd(II)/carboxylate system, the coordination number of Cd(II) can vary from 4 to 8, depending on the coordination ability of the carboxylate ligand. Thus, in order to get better results, it is necessary to control the PH value in the range of ca. 4–9.

In general, the Rb^+ has a strong tendency to form a cation hydration complex, acting only as a counter ion when the reaction is carried out in aqueous solution, as usually happens in the hydrothermal synthesis where water is used as a reaction medium.¹ However, in the absence of water, it has a great opportunity to coordinate to carboxylate oxygen atoms and participate in the network construction. On the other hand, for most of the Cd(II)/carboxylate frameworks synthesized under hydrothermal conditions, the Cd(II) center is usually 6-coordinate, chelated by two carboxylate groups, leaving two coordination sites to be occupied by solvent molecules (water in most cases) or nitrogen atoms from auxiliary ligands. When the reaction is carried out in organic solvent without adding any auxiliary ligands, the Cd(II) ion is able to coordinate to four carboxylate groups, leading to a 8-coordinate structure. However, in this case, the final product would be an anionic framework and an appropriate cation is needed. Based on the above considerations, we use DMF as a reaction medium because under solvothermal conditions, it can automatically control the

base/acid balance of the solution by releasing dimethylamine and at the same time produces $(\text{Me}_2\text{NH}_2)^+$ which can neutralize the overall charge in the anionic framework and serve as a cation template.

When Rb is replaced by Li, a known compound with different structure was made.² By Na and K, isomorphous crystals $[\text{M}_2\text{Cd}_3(\text{OBA})_4(\text{H}_2\text{O})_2(\text{DMF})_2] \cdot (\text{H}_2\text{O})_2$ (M = Na, K) whose structures are different from that of **1** were isolated.³ With Cs ion, no product was isolated. In these compounds, the alkali metal ions not only serve as counter ions, but also as nodes to extend the framework structures.

The IR spectrum of **1** shows the characteristic bands of the carboxylic groups in the usual region at $1463\text{--}1317\text{ cm}^{-1}$ for the symmetric vibrations and at $1651\text{--}1482\text{ cm}^{-1}$ for the asymmetric vibrations (Fig. S6). The absence of strong absorption associated with the carboxyl group at around 1701 cm^{-1} indicates that the H_2OBA ligand in **1** is completely deprotonated.

In order to investigate the UV stability of the title compound, XRD, luminescent, IR and UV-adsorption spectra for the as-synthesized and UV treated sample (under excited by the portable UV lamp for 2 h) were conducted (Fig. S9). No obvious change has been observed before and after excited by the UV light, which demonstrates the UV stability of the compound.

The excitation spectra for 427 and 566 nm emissions present two major bands centered at 304 nm in the high-energy region and at 400 nm in the low-energy area (Fig. S10). The overlap of two bands may indicate the coexistence of ILCT ($\pi \rightarrow \pi^*$) and LMCT transitions.⁴⁻⁶

Reference:

1. S. M. Humphrey, R. A. Mole, R. I. Thompson, and P. T. Wood. *Inorg. Chem.* 2010, **49**, 3441–3448.
2. J. D. Lin, X. F. Long, P. Lin, and S. W. Du. *Cryst. Growth Des.*, 2010, **10**, 146–157.
3. Unpublished results
4. (a) Y. Sun, K. Ye, H. Zhang, J. Zhang, L. Zhao, B. Li, G. Yang, B. Yang, Y. Wang, S. W. Lai, and C. M. Che. *Angew. Chem. Int. Ed.* 2006, **45**, 5610–5613. (b) K. Jayaramulu, P. Kanoo, S. J. George and T. K. Maj. *Chem. Commun.*, 2010, **46**, 7906–7908. (c) Y. Takashima, V. M. Martínez, S. Furukawa, M. Kondo, S.

Shimomura, H. Uehara, M. Nakahama, K. Sugimoto, S. Kitagawa, *Nat. Commun.*, DOI: 10.1038/ncomms1170. (d) H. L. Jiang, Y. Tatsu, Z. H. Lu, and Q. Xu *J. Am. Chem. Soc.* 2010, **132**, 5586–5587. (e) M. Xue, G. Zhu, Y. Zhang, Q. Fang, I. J. Hewitt, S. Qiu. *Cryst. Growth Des.*, 2008, **8**, 427–434.

5. (a) Y. Qiu, Y. Li, G. Peng, J. Cai, L. Jin, L. Ma, H. Deng, M. Zeller, and S. R. Batten. *Cryst. Growth Des.*, 2010, **10**, 1332-1340. (b) Q. Zhu, T. Sheng, C. Tan, S. Hu, R. Fu, and X. Wu. *Inorg. Chem.* 2011, **50**, 7618–7624. (c) J. C. Dai, X. T. Wu, Z. Y. Fu, C. P. Cui, S. M. Hu, W. X. Du, L. M. Wu, H. H. Zhang, R. Q. Sun. *Inorg. Chem.* 2002, **41**, 1391–1396

6. Y. Cui, Y. Yue, G. Qian, and B. Chen. *Chem. Rev.* 2012, **112**, 1126–1162.

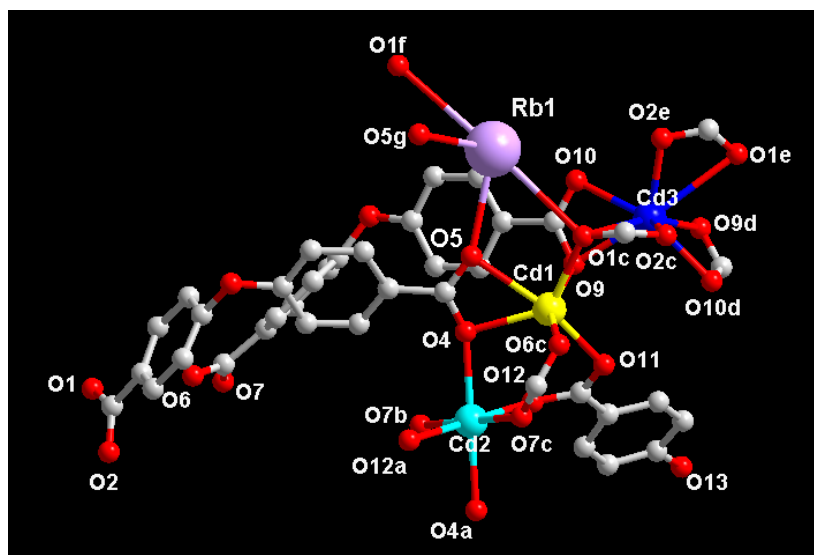


Fig. S1 The coordination environment of metal centers in compound **1**. H atoms were omitted for clarity. Symmetry codes: (a) $1-x, -y, -z$, (b) $x, 0.5-y, 0.5-z$. (c) $1-x, -0.5+y, -0.5+z$. (d) $0.5-x, -y, z$. (e) $-0.5+x, 0.5-y, -0.5+z$. (f) $1-x, 1-y, -z$. (g) $x, 0.5-y, -0.5-z$.

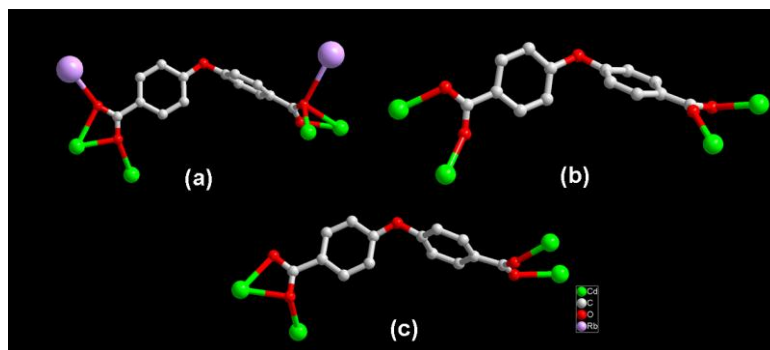


Fig. S2 The coordination environment of ligands in compound **1**.

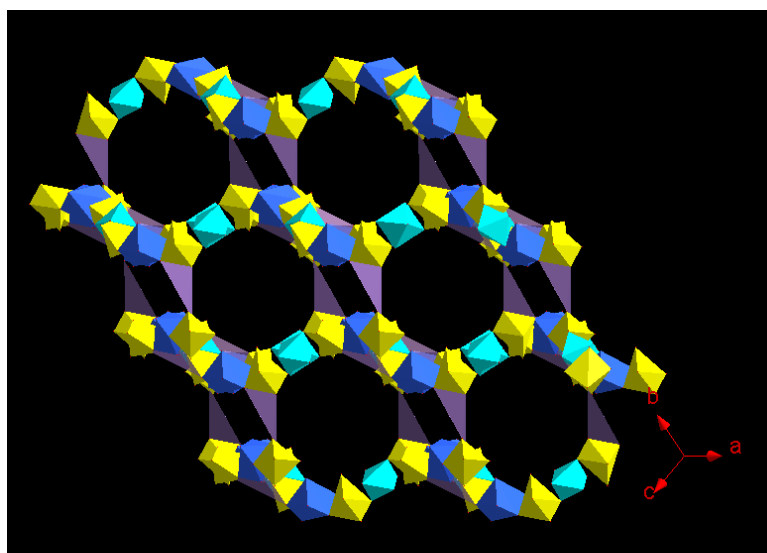


Fig. S3 View of the 3D inorganic network from the [1 1 1] direction.

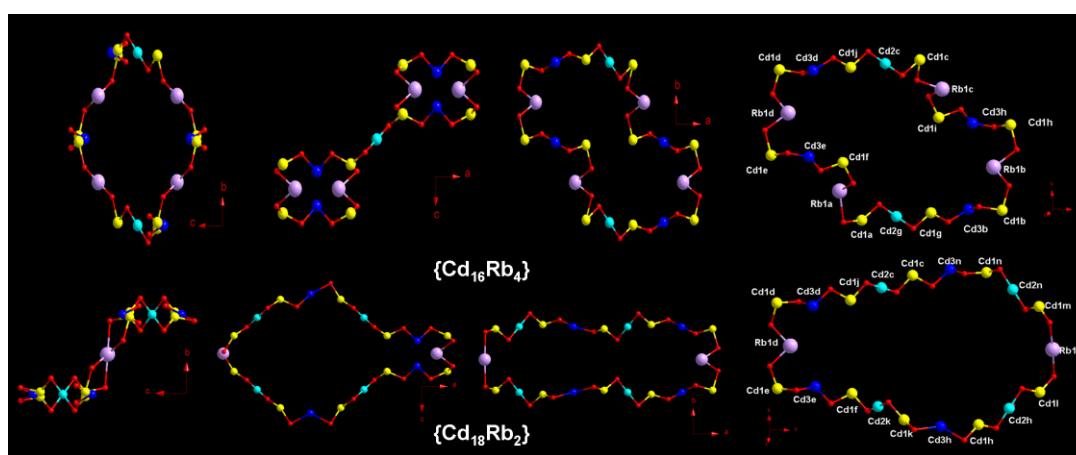


Fig. S4 View of {Cd₁₆Rb₄} and {Cd₁₈Rb₂} rings along separated axes. (a) $0.5 + x, y, -z$. (b) $1 + x, y, z$. (c) $1.5 - x, 1 - y, z$. (d) $1 - x, 1 - y, -z$. (e) $1 - x, 0.5 + y, 0.5 + z$. (f) $0.5 + x, 0.5 - y, 0.5 + z$. (g) $1.5 - x, -y, z$. (h) $1 + x, 0.5 - y, -0.5 - z$. (i) $1.5 - x, 0.5 + y, -0.5 - z$. (j) $0.5 + x, 1 + y, -z$. (k) $1.5 - x, 0.5 + y, -0.5 - z$. (l) $2 - x, 0.5 + y, 0.5 + z$. (m) $2 - x, 1 - y, -z$. (n) $1 + x, 1 + y, z$.

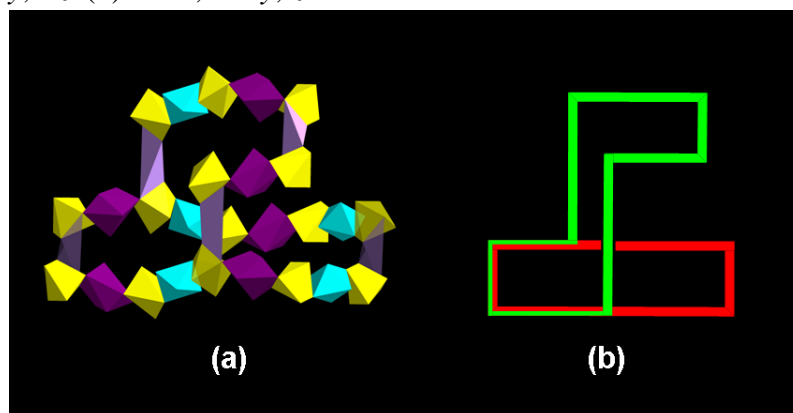


Fig. S5 A polyhedral view (a) and a schematic representation (b) of {Cd₁₆Rb₄} and {Cd₁₈Rb₂} rings.

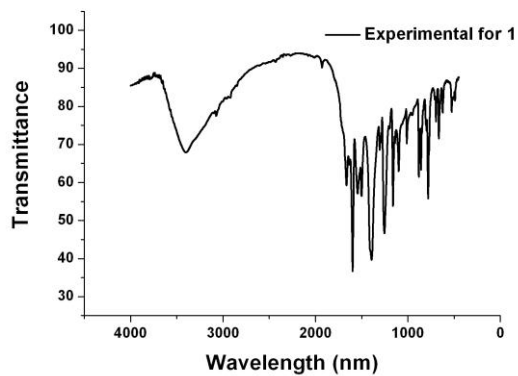


Fig. S6 IR spectrum of compound **1**.

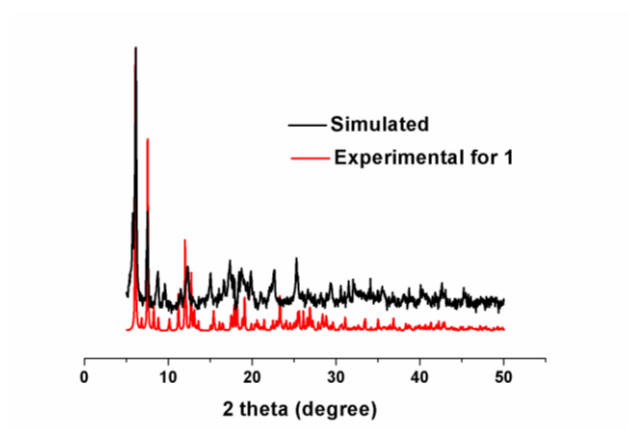


Fig. S7. Simulated and experimental XRD powder patterns for compound **1**.

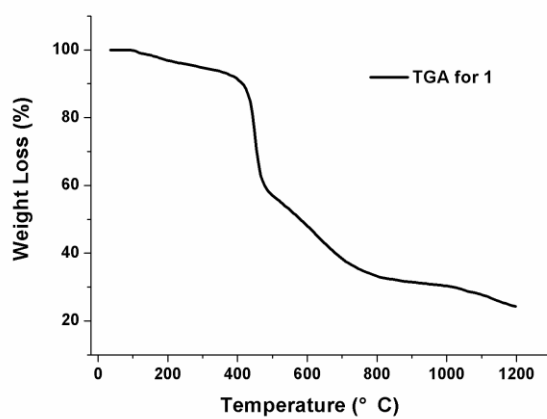


Fig. S8. TGA diagram for compound **1**.

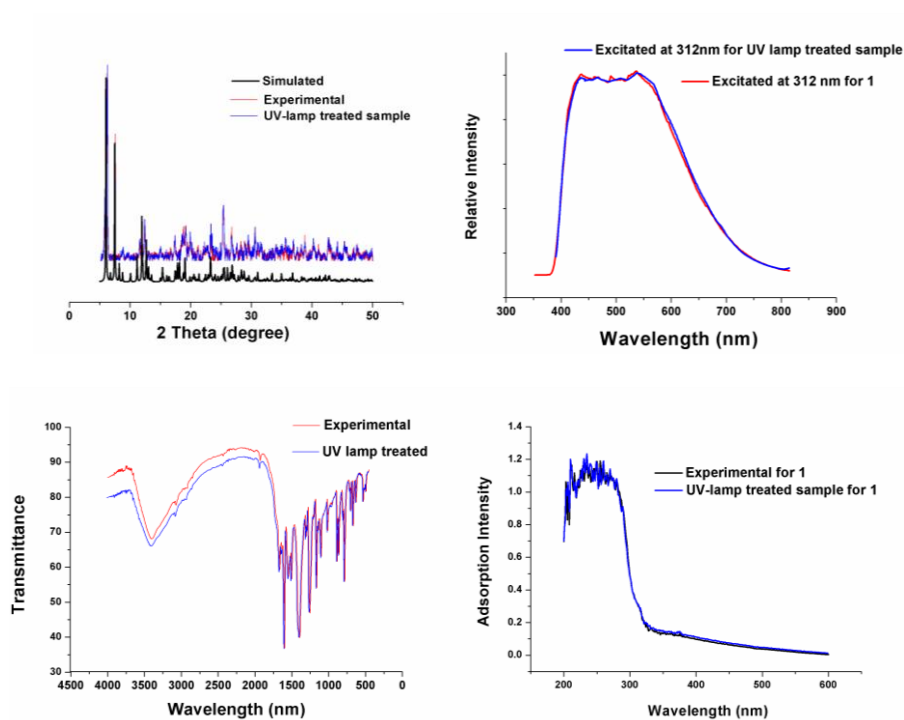


Fig. S9 XRD, luminescent, IR and UV-adsorption spectra of compound **1** before and after excited by the portable UV-lamp for 2 h.

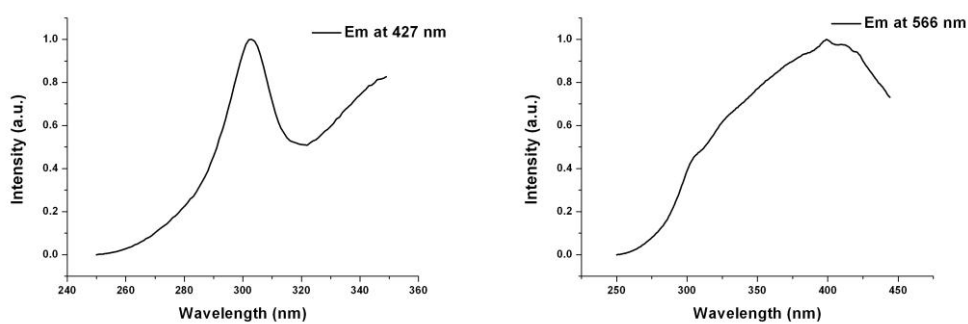


Fig. S10 Excitation spectra for the emissions at 427 and 566 nm in the solid state.

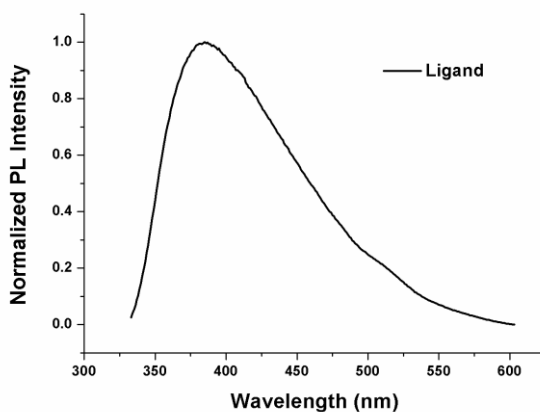


Fig. S11 The luminescence spectrum of the ligand (H_2OBA) at room temperature.

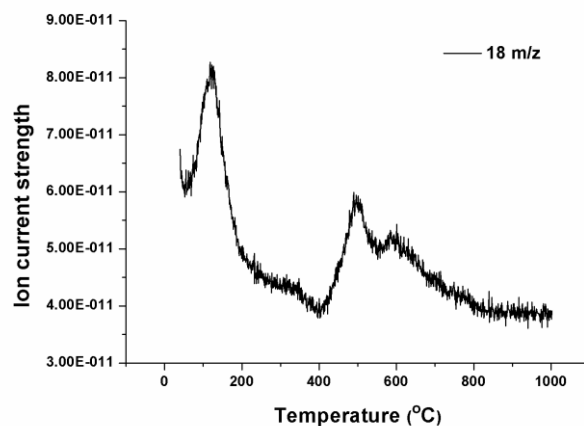


Fig. S12 MS analysis of **1** with ion current signals for $m/z = 18$.

Table S1. Pertinent Crystal Data and Structure Refinement Results for **1**.

Compound	1
CCDC	912851
Formula	$C_{72}H_{50}Cd_4NO_{26} Rb$
M ($g\ mol^{-1}$)	1880.24
Crystal system	Orthorhombic
Space group	<i>Pnna</i>
a (Å)	26.092(7)
b (Å)	15.839(4)
c (Å)	17.659(5)
V (Å ³)	7298(3)
Z	4
D_c ($g\ cm^{-3}$)	1.711
μ (mm^{-1})	1.893
$F(000)$	3704
GOF	1.135
R_1^a	0.0756
wR_2^a	0.2409

$$^aR = \sum (||F_o| - |F_c||) / \sum |F_o|, wR = \{ \sum w[(F_o^2 - F_c^2)^2] / \sum w[(F_o^2)^2] \}^{1/2}; [F_o > 4(F_c)].$$

Table S2 The CIE coordinates of emissions excited at different wavelengths.

Excitation (nm)	CIE	
	<i>x</i>	<i>y</i>
300	0.26	0.27
304	0.26	0.28
308	0.28	0.3
312	0.3	0.33
316	0.3	0.35
320	0.31	0.36
324	0.31	0.36
328	0.31	0.35
332	0.31	0.35
336	0.31	0.35
340	0.31	0.35
344	0.31	0.35
348	0.31	0.35